THE JOURNAL OF PHYSICAL CHEMISTRY LETTERS
A JOURNAL OF THE AMERICAN CHEMICAL SOCIETY

pubs.acs.org/JPCL

Letter

# The Photocycle of Bacteriophytochrome Is Initiated by Counterclockwise Chromophore Isomerization

Dmitry Morozov, Vaibhav Modi, Vladimir Mironov, and Gerrit Groenhof*

Cite This: *J. Phys. Chem. Lett.* 2022, 13, 4538–4542

Read Online

ACCESS | Metrics & More | Article Recommendations | Supporting Information

**ABSTRACT:** Photoactivation of bacteriophytochrome involves a cis−trans photoisomerization of a biliverdin chromophore, but neither the precise sequence of events nor the direction of the isomerization is known. Here, we used nonadiabatic molecular dynamics simulations on the photosensory protein dimer to resolve the isomerization mechanism in atomic detail. In our simulations the photoisomerization of the D ring occurs in the counterclockwise direction. On a subpicosecond time scale, the photoexcited chromophore adopts a short-lived intermediate with a highly twisted configuration stabilized by an extended hydrogen-bonding network. Within tens of picoseconds, these hydrogen bonds break, allowing the chromophore to adopt a more planar configuration, which we assign to the early Lumi-R state. The isomerization process is completed via helix inversion of the biliverdin chromophore to form the late Lumi-R state. The mechanistic insights into the photoisomerization process are essential to understand how bacteriophytochrome has evolved to mediate photoactivation and to engineer this protein for new applications.

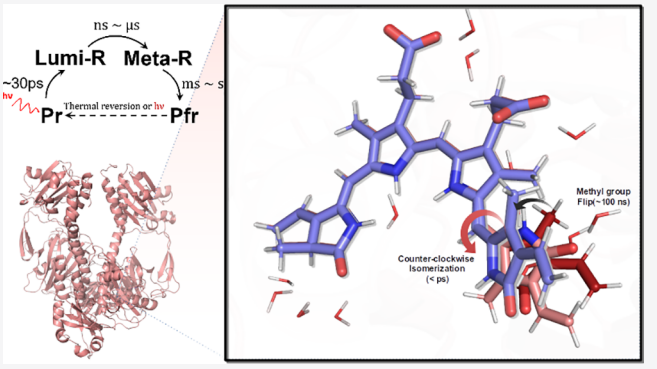


Phytochrome is a photoreceptor protein in plants, fungi, and bacteria that mediates the response of these organisms to red and far-red light.[1−8] Upon photoactivation, the protein dimer interconverts reversibly between a red ($P_r$) and a far-red ($P_{fr}$) absorbing state.[7,9] Time-resolved wide-angle X-ray scattering of the photosensory domain suggests significant structural changes between these states[10] that control the activity of a histidine kinase (HK) domain.[11−13] Based on X-ray structures of the $P_r$ and $P_{fr}$ conformations of the photosensory unit (i.e., the protein without the HK domain),[10,14] the first step in this signal transduction pathway is assumed to be the photoisomerization of a covalently bound tetrapyrrole biliverdin chromophore (Figure 1a), but the exact mechanism is not known. On the basis of changes in circular dichroism between the $P_r$ and $P_{fr}$ states of phytochromes from various organisms, Lagarias and co-workers proposed that the isomerization proceeds counterclockwise in the *phytobilin* phytochromes of plants and cyanobacteria but clockwise in the *biliverdin* phytochrome of bacteria and fungi.[15] In contrast, recent time-resolved serial femtosecond X-ray diffraction (trSFX) experiments on the chromophore binding domain (CBD) of the *Deinococcus radiodurans* phytochrome (DrBphP) suggest a counterclockwise photoisomerization of the biliverdin chromophore binding phytochromes.[16]

In the trSFX experiments on the CBD of DrBphP two snapshots of what is essentially a dynamic process that spans multiple time scales, were captured at pump−probe delays of 1 and 10 ps.[16] The pump laser, with which the photoisomerization was initiated, had high power, and some of the structural changes may therefore have been induced by multiphoton absorption. To investigate the photoisomerization mechanism in the single-photon excitation regime, we resort to nonadiabatic molecular dynamics simulations. While the accuracy of atomistic computer simulations remains a matter of concern despite the tremendous progress in hardware and software, we note that our previous simulations correctly predicted the sequence of events in the photoisomerization process in a related protein.[17,18]

Here, we used the same hybrid quantum mechanics/molecular mechanics (QM/MM) approach[19,20] to follow the photoinduced dynamics in the complete photosensory dimer (CBD-PHY) of DrBphP.[10] In our QM/MM model,[21] one biliverdin chromophore was described at the SA2-CASSCF-(6,6)/3-21G level of theory,[22] while the rest of the system, including the rest of the monomer as well as the complete other monomer, waters, and ions were treated with the Amber03 force field.[23] All details of the nonadiabatic simulations are provided as Supporting Information, including

**Received:** March 28, 2022
**Accepted:** May 13, 2022
**Published:** May 16, 2022

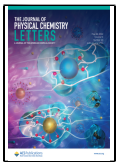







https://doi.org/10.1021/acs.jpclett.2c00899
*J. Phys. Chem. Lett.* 2022, 13, 4538–4542

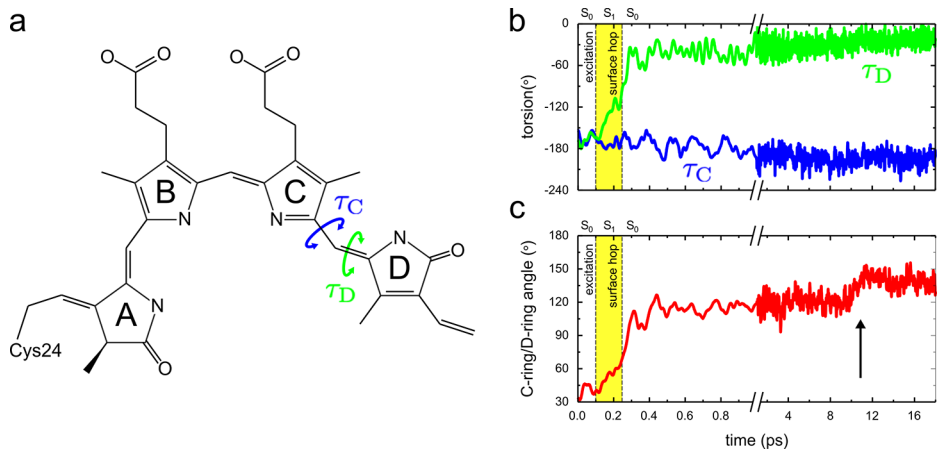


**Figure 1.** (a) Schematic representation of the biliverdin chromophore in DrBphP. The rings are labeled A, B, C, and D. The torsion angles for $\tau_C$ and $\tau_D$ are highlighted. (b) Time evolution of torsions $\tau_C$ and $\tau_D$. Note the change in the scale on the time axis at 1 ps. The yellow background indicates that the system is in the electronic excited state ($S_1$). (c) Angle between the normals of the C and D rings. The vertical arrow indicates a structural relaxation of the chromophore (see Figure 3).

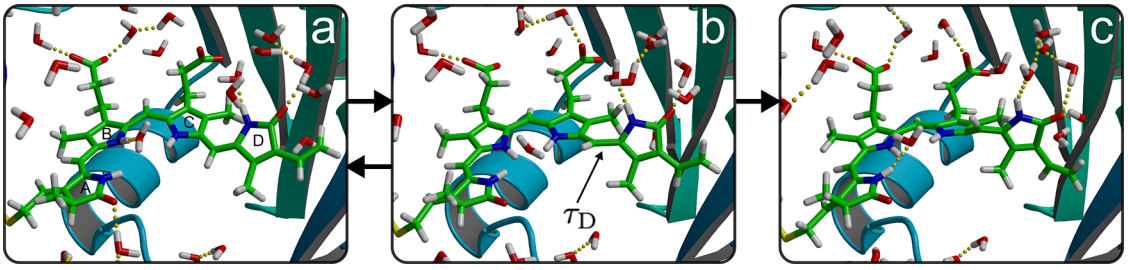


**Figure 2.** (a) Snapshot at the start of a simulation. The chromophore is in the ZZZssa configuration. (b) Snapshot when the trajectory reaches the $S_1/S_0$ conical intersection hyperline. The $\tau_D$ torsion (arrow) is around 90° (Figure 1b). (c) Snapshot at 1 ps after excited-state decay through the conical intersection. Both $\tau_C$ and $\tau_D$ are close to their equilibrium values, but the D ring is still twisted with respect to the C ring and the rest of the chromophore (Figure 1c). This strained configuration is stabilized by a hydrogen bond network between the D ring nitrogen and carboxyl oxygen atoms, on the one hand, and buried water molecules, on the other hand.

a validation of our model at the correlated xMCQDPT2/SA3-CASSCF(12,12)/cc-pVDZ level of theory.[24]

Immediately after resonant photoexcitation to the excited state ($S_1$) potential energy surface, the chromophore relaxes on a subpicosecond time scale from the Franck−Condon region to the conical intersection seam between the ground state ($S_0$) and excited state in 33 out of 50 simulations (Table S1, Supporting Information). Upon reaching the $S_1/S_0$ conical intersection, the system decays to the ground state. In four trajectories, the chromophore reaches a new configuration (discussed below), while in the other 29 trajectories, the chromophore rapidly relaxes back into the original ZZZssa geometry, in line with the very low quantum yield of photoactivation in bacterial phytochromes.[25−27] In 17 out of 50 simulations, the chromophore remains planar and does not decay to $S_0$ on the 5 ps time scale of the simulation. Although 5 ps is orders of magnitude shorter than the measured excited-state lifetime of CBD-PHY (170 ps),[28] we speculate nevertheless that these trajectories represent longer-lived substates in the protein conformational ensemble that are responsible for fluorescence.

In Figure 1, we show the evolution of the angle between the normal of the C ring and the normal of the D ring as well as of the $\tau_C$ and $\tau_D$ torsions in one of the trajectories that forms a photoproduct. In the 33 trajectories that reach the conical intersection, the initial relaxation process is highly similar and proceeds via twisting the $\tau_D$ torsion angle to about 90° (Figures 1b and 2b). Along this reaction coordinate, the gap between the $S_0$ and $S_1$ states decreases until it disappears at the $S_1/S_0$ intersection (Figures S3 and S4), where a diabatic surface hop takes the system back to the electronic ground state. The excited-state decay process in these 33 trajectories takes less than a picosecond on average (Table S1), which is in line with recent simulations of the CBD monomer,[29] but seems to contradict the 170 ps excited-state lifetime measured experimentally for this system.[28] We note, however, that the excited-state decay in phytochromes is a highly heterogeneous process and that fits to the excited-state lifetime in pump−probe experiments require multiple components,[27,28,30−36] including an ultrafast subpicosecond component.[25,28,37] We therefore tentatively assign this subpicosecond component to the ultrafast photoinduced rotation of the D ring and attribute the slower components to the protein conformations, in which the chromophore remains planar without deactivating (Table S1).

After the radiationless decay from the excited state, the $\tau_D$ torsion angle reverts back in 29 trajectories, restoring the ZZZssa configuration of the chromophore. In the other four trajectories, the $\tau_D$ torsion angle rotates further on the ground state to reach a ZZEssa configuration (Figure 2b). This configuration is, however, strained, as indicated by an almost perpendicular orientation of the D ring with respect to the rest of the chromophore in Figure 2c. In this configuration, which we term $I_0$, the angle between the C and D rings is around



https://doi.org/10.1021/acs.jpclett.2c00899
J. Phys. Chem. Lett. 2022, 13, 4538−4542

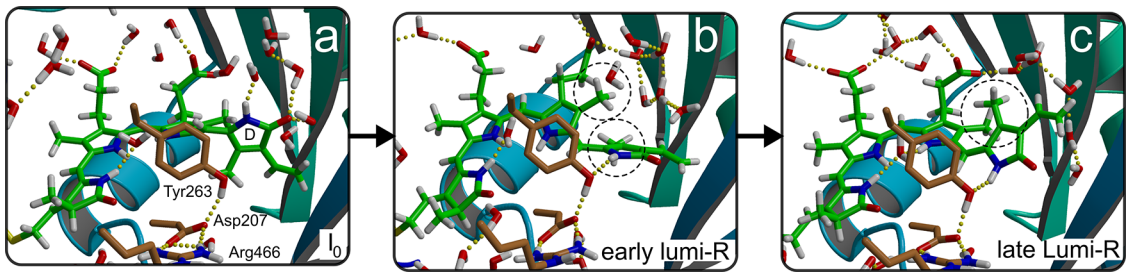


**Figure 3.** (a) Configuration in the first local minimum on $S_0$ after decay from $S_1$ ($I_0$, same as Figure 2c but with additional structural details). The chromophore is twisted with the D ring almost perpendicular to the C ring and the rest of the chromophore. The D ring forms an extensive hydrogen-bonding network involving multiple buried water molecules. (b) Configuration after 15 ps. The D ring is more planar with respect to the rest of the chromophore and donates a hydrogen bond to the hydroxyl group of Tyr263. The latter configuration is further stabilized by a hydrogen-bonding network involving Asp207 and Arg466. We assign this configuration to the early Lumi-R state in the photocycle. The circles emphasize the relative positions of the methyl substituents of the C and D rings. (c) Configuration after flipping the methyl groups of the C and D ring in umbrella sampling simulations (see the Supporting Information for details). We assign this configuration, in which the D ring has undergone a 180° rotation with respect to the $P_r$ resting state, to the late Lumi-R state.[38]

120° and remains at that angle for at least 10 ps (Figure 1c). As shown in Figure 2c, a hydrogen-bonding network that involves multiple buried water molecules stabilizes the D ring in this orientation, with the amino (N−H) and carboxyl (C═O) groups acting as donor and acceptor, respectively. The formation of this twisted configuration on a subpicosecond time scale is supported both by time-resolved X-ray crystallography, which resolved such twisted structure on similar time scales,[16] and by femtosecond stimulated Raman spectroscopy,[37] which probed the rise of signals associated with out-of-plane distortions, with a 450 fs time constant. A comparison between the twisted intermediate found in our simulations and the 1 ps structure refined by Claesson et al.[16] in Figure S10 reveals that the simulations predict a very similar chromophore configuration but not the large displacement of the pyrrole water molecule. We speculate therefore that the photodissociation of the pyrrole water observed in trSFX might have been induced by a multiphoton absorption process due to the very high laser power in the experiments.

Eventually, the hydrogen-bonding network breaks up in the QM/MM simulations, and the chromophore relaxes into a more planar configuration, as shown by the transition around 11 ps in Figure 1c. In this configuration, which is stable throughout the rest of the simulation, the chromophore is further stabilized by a new hydrogen bond between the D ring amino group (N−H) and the hydroxyl group of the conserved Tyr263 (Figure 3). Because mutating this residue into a phenylalanine hinders the formation of Lumi-R,[39] we attribute the configuration in Figure 3b to the early Lumi-R state, which is also observed on similar time scales in transient absorption spectroscopy experiments.[28] Statistically, the number of trajectories is small but nevertheless yields a consistent picture of the photoisomerization mechanism.

Although the early Lumi-R intermediate is stable in the rest of the MD simulations, the chromophore is not in the configuration observed in the X-ray structure of the activated $P_{fr}$ state.[14] The main difference is the facial disposition of the D ring relative to the C ring:[15] In the $P_{fr}$ X-ray structure the D ring adopts a $\beta_f$ disposition, in which the methyl group of the D ring is *above* the plane of the C ring (Figure 3c),[14] while in our early Lumi-R intermediate, the disposition of the D ring is $\alpha_f$ with its methyl substituent lying *below* the plane of the C ring (Figures 2c and 3b). To estimate the free energy barrier associated with changing the disposition of the D ring from $\alpha_f$ to $\beta_f$ within the protein environment, we performed umbrella sampling simulations[40] at the PBE/DZVP//Amber03 level of theory (see the Supporting Information for details). The results of these simulations, shown in Figure S8, suggest an upper bound of 33 kJ $mol^{-1}$ for the barrier separating the $\alpha_f$ and $\beta_f$ dispositions of the D ring. Thus, based on Eyring's transition state theory (TST), the time scale of this inversion process would be on the order of 62 ns, which is much faster than the onset of the large protein structural changes seen in time-resolved WAXS experiments[10] but qualitatively in line with the time scales at which a late Lumi-R state was observed in transient infrared (trIR) spectroscopy measurements.[38,41] We therefore tentatively assign the structure in which the chromophore has already adopted the configuration of the $P_{fr}$ state (i.e., the ZZEssa configuration with the $\beta_f$ disposition of the D ring), while the protein is still in the $P_r$ conformation, to the late Lumi-R intermediate in the photocycle (Figure 3c).

Because in a circular dichroism spectrum (CD) the Q-band absorption of the chromophore has a negative rotation in the $\alpha_f$ disposition, but a positive rotation in the $\beta_f$ disposition,[42−44] and the CD of this Q-band is negative in both the $P_r$ and $P_{fr}$ states, Rockwell et al. proposed a clockwise photoisomerization of the D ring.[15] In contrast, our simulations suggest a counterclockwise rotation of the D ring, which was also observed in the simulations by Salvadori et al.[29] To investigate the effect of the counterclockwise isomerization on the CD signal, we computed CD spectra of the $P_r$ state and the structural intermediates (details in the Supporting Information). While the rotation of Q-band is negative in $P_r$, late Lumi-R, and $P_{fr}$, it is positive in the early Lumi-R intermediate (Figure S9). Thus, to verify the validity of our results, we propose to transiently probe the effects of photoabsorption on the CD spectrum with picosecond time resolution, as has been done by Mendonça and co-workers for the photoactive yellow protein.[45]

Summarizing, the results of our nonadiabatic MD simulations suggest a counterclockwise photoisomerization of the biliverdin chromophore in the phytochrome of *Deinococcus radiodurans*, which proceeds via three intermediates: $I_0$, early Lumi-R, and late Lumi-R. Although the structures of these intermediates have so far not been resolved experimentally, their lifetimes are in reasonable agreement with experimental estimates.[12,37,38] Because already in the late Lumi-R intermediate the chromophore has the same configuration as in the $P_{fr}$ state, while the rest of the protein still adopts the $P_r$ conformation, we speculate that complete chromophore



https://doi.org/10.1021/acs.jpclett.2c00899
J. Phys. Chem. Lett. 2022, 13, 4538−4542

isomerization is essential to trigger the conformational changes. The atomistic insights into the dynamics and interactions of the isomerization process may be useful to systematically improve phytochromes for new applications, such as optogenetics,[46,47] or fluorescence microscopy.[47,48]

## ■ ASSOCIATED CONTENT

### Supporting Information

The Supporting Information is available free of charge at https://pubs.acs.org/doi/10.1021/acs.jpclett.2c00899.

Complete description of the QM/MM simulations and other calculations, overviews of nonadiabatic simulations, calculated circular dichroism spectra, and comparisons of structural intermediates to time-resolved X-ray structures (PDF)

Movie S1 (MOV)

Movie S2 (MOV)

Movie S3 (MOV)

Transparent Peer Review report available (PDF)

## ■ AUTHOR INFORMATION


### Corresponding Author

**Gerrit Groenhof** − *Nanoscience Center and Department of Chemistry, University of Jyväskylä, 40014 Jyväskylä, Finland;* orcid.org/0000-0001-8148-5334; Email: gerrit.x.groenhof@jyu.fi

### Authors

**Dmitry Morozov** − *Nanoscience Center and Department of Chemistry, University of Jyväskylä, 40014 Jyväskylä, Finland;* orcid.org/0000-0001-9524-948X

**Vaibhav Modi** − *Nanoscience Center and Department of Chemistry, University of Jyväskylä, 40014 Jyväskylä, Finland;* orcid.org/0000-0002-9309-0409

**Vladimir Mironov** − *Department of Chemistry, Kyungpook National University, Daegu 702-701, South Korea;* orcid.org/0000-0002-9454-5823

Complete contact information is available at: https://pubs.acs.org/10.1021/acs.jpclett.2c00899


### Author Contributions

D.M. and V.M. contributed equally to this work.


### Funding

This work has been done as part of the BioExcel CoE (www.bioexcel.eu), a project funded by the European Union Contracts H2020-INFRAEDI-02-2018-823830 and H2020-EINFRA-2015-1-675728. In addition, the work received support from the Academy of Finland (Grants 332743 and 324975).


### Notes

The authors declare no competing financial interest.

## ■ ACKNOWLEDGMENTS


We thank Janne Ihalainen and Heikki Takala for valuable discussions. We thank the Finnish Grid and Cloud Infrastructure (persistent identifier urn:nbn:fi:research-infras-2016072533), the CSC-IT center in Espoo, Finland, and PRACE (DECI-13) for awarding us access to resources at Cartesius in Dutch facility SURFsara.


## ■ REFERENCES


(1) Sineshchekov, V. A. Photobiophysics and photobiochemistry of the heterogeneous phytochrome system. *Biochim. Biophys. Acta - Bioenerg.* **1995**, *1228*, 125−164.

(2) Hughes, J.; Lamparter, T.; Mittmann, F.; Hartmann, E.; Gärtner, W.; Wilde, A.; Börner, T. A prokaryotic phytochrome. *Nature* **1997**, *386*, 663−663.

(3) Yeh, K.-C.; Wu, S.-H.; Murphy, J. T.; Lagarias, J. C. A cyanobacterial phytochrome two-component light sensory system. *Science* **1997**, *277*, 1505−1508.

(4) Davis, S. J.; Vener, A. V.; Vierstra, R. D. Bacteriophytochromes: Phytochrome-Like Photoreceptors from Nonphotosynthetic Eubacteria. *Science* **1999**, *286*, 2517−2520.

(5) Jiang, Z.; Swem, L. R.; Rushing, B. G.; Devanathan, S.; Tollin, G.; Bauer, C. E. Bacterial photoreceptor with similarity to photoactive yellow protein and plant phytochromes. *Science* **1999**, *285*, 406−409.

(6) Smith, H. Phytochromes and light signal perception by plants−an emerging synthesis. *Nature* **2000**, *407*, 585−591.

(7) Rockwell, N. C.; Su, Y.-S.; Lagarias, J. C. Phytochrome structure and signaling mechanisms. *Annu. Rev. Plant Biol.* **2006**, *57*, 837−858.

(8) Möglich, A.; Yang, X.; Ayers, R. A.; Moffat, K. Structure and function of plant photoreceptors. *Annu. Rev. Plant Biol.* **2010**, *61*, 21−47.

(9) Rockwell, N. C.; Lagarias, J. C. The structure of phytochrome: a picture is worth a thousand spectra. *Plant Cell* **2006**, *18*, 4−14.

(10) Takala, H.; Bjorling, A.; Berntsson, O.; Lehtivuori, H.; Niebling, S.; Hoernke, M.; Kosheleva, I.; Henning, R.; Menzel, A.; Ihalainen, J. A.; Westenhoff, S. Signal amplification and transduction in phytochrome photosensors. *Nature* **2014**, *509*, 245.

(11) Bhoo, S.; Davis, S.; Walker, J.; Karniol, B.; Vierstra, R. Bacteriophytochromes are photochromic histidine kinases using a biliverdin chromophore. *Nature* **2001**, *414*, 776−779.

(12) Björling, A.; Berntsson, O.; Lehtivuori, H.; Takala, H.; Hughes, A. J.; Panman, M.; Hoernke, M.; Niebling, S.; Henry, L.; Henning, R.; et al. Structural photoactivation of a full-length bacterial phytochrome. *Sci. Adv.* **2016**, *2*, e1600920.

(13) Multamäki, E.; Nanekar, R.; Morozov, D.; Lievonen, T.; Golonka, D.; Wahlgren, W. Y.; Stucki-Buchli, B.; Rossi, J.; Hytönen, V. P.; Westenhoff, S.; Ihalainen, J. A.; Möglich, A.; Takala, H. Comparative analysis of two paradigm bacteriophytochromes reveals opposite functionalities in two-component signaling. *Nat. Commun.* **2021**, *12*, 4394.

(14) Burgie, E. S.; Zhang, J.; Vierstra, R. D. Crystal structure of Deinococcus phytochrome in the photoactivated state reveals a cascade of structural rearrangements during photoconversion. *Structure* **2016**, *24*, 448−457.

(15) Rockwell, N. C.; Shang, L.; Martin, S. S.; Lagarias, J. C. Distinct classes of red/far-red photochemistry within the phytochrome superfamily. *Proc. Natl. Acad. Sci. U. S. A.* **2009**, *106*, 6123−6127.

(16) Claesson, E.; Wahlgren, W. Y.; Takala, H.; Pandey, S.; Castillon, L.; Kuznetsova, V.; Henry, L.; Panman, M.; Carrillo, M.; Kübel, J.; et al. The primary structural photoresponse of phytochrome proteins captured by a femtosecond X-ray laser. *Elife* **2020**, *9*, e53514.

(17) Groenhof, G.; Bouxin-Cademartory, M.; Hess, B.; De Visser, S. P.; Berendsen, H. J.; Olivucci, M.; Mark, A. E.; Robb, M. A. Photoactivation of the photoactive yellow protein: why photon absorption triggers a trans-to-cis isomerization of the chromophore in the protein. *J. Am. Chem. Soc.* **2004**, *126*, 4228−4233.

(18) Pande, K.; Hutchison, C. D.; Groenhof, G.; Aquila, A.; Robinson, J. S.; Tenboer, J.; Basu, S.; Boutet, S.; DePonte, D. P.; Liang, M.; et al. Femtosecond structural dynamics drives the trans/cis isomerization in photoactive yellow protein. *Science* **2016**, *352*, 725−729.

(19) Warshel, A.; Levitt, M. Theoretical studies of enzymic reactions: dielectric, electrostatic and steric stabilization of the carbonium ion in the reaction of lysozyme. *J. Mol. Biol.* **1976**, *103*, 227−249.

(20) Boggio-Pasqua, M.; Burmeister, C. F.; Robb, M. A.; Groenhof, G. Photochemical reactions in biological systems: probing the effect

of the environment by means of hybrid quantum chemistry/molecular mechanics simulations. *Phys. Chem. Chem. Phys.* **2012**, *14*, 7912−7928.
(21) Modi, V.; Donnini, S.; Groenhof, G.; Morozov, D. Protonation of the Biliverdin IXα Chromophore in the Red and Far-Red Photoactive States of a Bacteriophytochrome. *J. Phys. Chem. B* **2019**, *123*, 2325−2334.
(22) Siegbahn, P. E. M.; Almlof, J.; Heiberg, A.; Roos, B. O. The complete active space SCF (CASSCF) method in a Newton−Raphson formulation with application to the HNO molecule. *J. Chem. Phys.* **1981**, *74*, 2384−2396.
(23) Duan, Y.; Wu, C.; Chowdhury, S.; Lee, M. C.; Xiong, G.; Zhang, W.; Yang, R.; Cieplak, P.; Luo, R.; Lee, T.; et al. A point-charge force field for molecular mechanics simulations of proteins based on condensed-phase quantum mechanical calculations. *J. Comput. Chem.* **2003**, *24*, 1999−2012.
(24) Granovsky, A. A. Extended multi-configuration quasi-degenerate perturbation theory: The new approach to multi-state multi-reference perturbation theory. *J. Chem. Phys.* **2011**, *134*, 214113.
(25) van Thor, J. J.; Ronayne, K. L.; Towrie, M. Formation of the Early Photoproduct Lumi-R of Cyanobacterial Phytochrome Cph1 Observed by Ultrafast Mid-Infrared Spectroscopy. *J. Am. Chem. Soc.* **2007**, *129*, 126−132.
(26) Lamparter, T.; Mittmann, F.; Gärtner, W.; Börner, T.; Hartmann, E.; Hughes, J. Characterization of recombinant phytochrome from the cyanobacterium Synechocystis. *Proc. Natl. Acad. Sci. U. S. A.* **1997**, *94*, 11792−11797.
(27) Toh, K. C.; Stojkovic, E. A.; van Stokkum, I. H. M.; Moffat, K.; Kennis, J. T. M. Proton-transfer and hydrogen-bond interactions determine fluorescence quantum yield and photochemical efficiency of bacteriophytochrome. *Proc. Natl. Acad. Sci. U. S. A.* **2010**, *107*, 9170−9175.
(28) Ihalainen, J. A.; Takala, H.; Lehtivuori, H. Fast photochemistry of canonical Bacteriophytochrome proteins - a species-specific comparison. *Front. Mol. Biosci.* **2015**, *2*, 75.
(29) Salvadori, G.; Macaluso, V.; Pellicci, G.; Cupellini, L.; Granucci, G.; Mennucci, B. Photochemistry and transient intermediates in a bacteriophytochrome photocycle revealed by multiscale simulations. *ChemRXiv* **2022**, 1−31.
(30) Toh, K. C.; Stojković, E. A.; Rupenyan, A. B.; van Stokkum, I. H. M.; Salumbides, M.; Groot, M.-L.; Moffat, K.; Kennis, J. T. M. Primary reactions of bacteriophytochrome observed with ultrafast mid-infrared spectroscopy. *J. Phys. Chem. A* **2011**, *115*, 3778−3786.
(31) Lehtivuori, H.; Rissanen, I.; Takala, H.; Bamford, J.; Tkachenko, N. V.; Ihalainen, J. A. Fluorescence properties of the chromophore-binding domain of bacteriophytochrome from Deinococcus radiodurans. *J. Phys. Chem. B* **2013**, *117*, 11049−11057.
(32) Kim, P. W.; Rockwell, N. C.; Freer, L. H.; Chang, C.-W.; Martin, S. S.; Lagarias, J. C.; Larsen, D. S. Unraveling the primary isomerization dynamics in cyanobacterial phytochrome Cph1 with multipulse manipulations. *J. Phys. Chem. Lett.* **2013**, *4*, 2605−2609.
(33) Kim, P. W.; Rockwell, N. C.; Martin, S. S.; Lagarias, J. C.; Larsen, D. S. Heterogeneous Photodynamics of the Pfr State in Cyanobacterial Phytochrome Cph1. *Biochemistry* **2014**, *53*, 4601−4611.
(34) Wang, C.; Flanagan, M. L.; McGillicuddy, R. D.; Zheng, H.; Ginzburg, A. R.; Yang, X.; Moffat, K.; Engel, G. S. Bacteriophytochrome Photoisomerization Proceeds Homoge- neously Despite Heterogeneity in Ground State. *Biophys. J.* **2016**, *111*, 2125−2134.
(35) Kirpich, J. S.; Mix, L. T.; Martin, S. S.; Rockwell, N. C.; Lagarias, J. C.; Larsen, D. S. Protonation Heterogeneity Modulates the Ultrafast Photocycle Initiation Dynamics of Phytochrome Cph1. *J. Phys. Chem. Lett.* **2018**, *9*, 3454−3462.
(36) Wang, D.; Qin, Y.; Zhang, M.; Li, X.; Wang, L.; Yang, X.; Zhong, D. The origin of ultrafast multiphasic dynamics in photoisomerization of bacteriophytochrome. *J. Phys. Chem. Lett.* **2020**, *11*, 5913−5919.
(37) Dasgupta, J.; Frontiera, R. R.; Taylor, K. C.; Lagarias, J. C.; Mathies, R. A. Ultrafast excited-state isomerization in phytochrome revealed by femtosecond stimulated Raman spectroscopy. *Proc. Natl. Acad. Sci. U. S. A.* **2009**, *106*, 1784−1789.
(38) Kübel, J.; Chenchiliyan, M.; Ooi, S. A.; Gustavsson, E.; Isaksson, L.; Kuznetsova, V.; Ihalainen, J. A.; Westenhoff, S.; Maj, M. Transient IR spectroscopy identifies key interactions and unravels new intermediates in the photocycle of a bacterial phytochrome. *Phys. Chem. Chem. Phys.* **2020**, *22*, 9195−9203.
(39) Takala, H.; Lehtivuori, H.; Berntsson, O.; Hughes, A.; Nanekar, R.; Niebling, S.; Panman, M. R.; Henry, L.; Menzel, A.; Westenhoff, S.; Ihalainen, J. A. On the (un)coupling of the chromophore, tongue interactions, and overall conformation in a bacterial phytochrome. *J. Biol. Chem.* **2018**, *293*, 8161−8172.
(40) Torrie, G.M.; Valleau, J.P. Non-physical sampling distributions in Monte-Carlo free energy estimation - umbrella sampling. *J. Comput. Phys.* **1977**, *23*, 187−199.
(41) Ihalainen, J. A.; Gustavsson, E.; Schroeder, L.; Donnini, S.; Lehtivuori, H.; Isaksson, L.; Thoing, C.; Modi, V.; Berntsson, O.; Stucki-Buchli, B.; Liukkonen, A.; Hakkanen, H.; Kalenius, E.; Westenhoff, S.; Kottke, T. Chromophore-protein interplay during the phytochrome photocycle revealed by step-scan FTIR spectroscopy. *J. Am. Chem. Soc.* **2018**, *140*, 12396−12404.
(42) Litts, J.; Kelly, J. M.; Lagarias, J. C. Structure-function studies on phytochrome. Preliminary characterization of highly purified phytochrome from Avena sativa enriched in the 124-kilodalton species. *J. Biol. Chem.* **1983**, *258*, 11025−11031.
(43) Borucki, B.; Otto, H.; Rottwinkel, G.; Hughes, J.; Heyn, M. P.; Lamparter, T. Mechanism of Cph1 phytochrome assembly from stopped-flow kinetics and circular dichroism. *Biochemistry* **2003**, *42*, 13684−13697.
(44) Seibeck, S.; Borucki, B.; Otto, H.; Inomata, K.; Khawn, H.; Kinoshita, H.; Michael, N.; Lamparter, T.; Heyn, M. P. Locked 5Zs-biliverdin blocks the Meta-RA to Meta-RC transition in the functional cycle of bacteriophytochrome Agp1. *FEBS Lett.* **2007**, *581*, 5425−5429.
(45) Mendonça, L.; Hache, F.; Changenet-Barret, P.; Plaza, P.; Chosrowjan, H.; Taniguchi, S.; Imamoto, Y. Ultrafast carbonyl motion of the photoactive yellow protein chromophore probed by femtosecond circular dichroism. *J. Am. Chem. Soc.* **2013**, *135*, 14637−14643.
(46) Gasser, C.; Taiber, S.; Yeh, C.-M.; Wittig, C. H.; Hegemann, P.; Ryu, S.; Wunder, F.; Möglich, A. Engineering of a red-light−activated human cAMP/cGMP-specific phosphodiesterase. *Proc. Natl. Acad. Sci. U. S. A.* **2014**, *111*, 8803−8808.
(47) Shcherbakova, D. M.; Shemetov, A. A.; Kaberniuk, A. A.; Verkhusha, V. V. Natural photoreceptors as a source of fluorescent proteins, biosensors, and optogenetic tools. *Annu. Rev. Biochem.* **2015**, *84*, 519−550.
(48) Piatkevich, K. D.; Suk, H.-J.; Kodandaramaiah, S. B.; Yoshida, F.; DeGennaro, E. M.; Drobizhev, M.; Hughes, T. E.; Desimone, R.; Boyden, E. S.; Verkhusha, V. V. Near-infrared fluorescent proteins engineered from bacterial phytochromes in neuroimaging. *Biophys. J.* **2017**, *113*, 2299−2309.


https://doi.org/10.1021/acs.jpclett.2c00899
J. Phys. Chem. Lett. 2022, 13, 4538−4542